

Terahertz resonant transmission through metallic mesh truss structures

Cite as: AIP Advances **9**, 125320 (2019); <https://doi.org/10.1063/1.5119385>

Submitted: 10 July 2019 • Accepted: 07 December 2019 • Published Online: 23 December 2019

Chul Kang,  Seong Han Kim, Gyuseok Lee, et al.



View Online



Export Citation



CrossMark

ARTICLES YOU MAY BE INTERESTED IN

[Strong emission of THz radiation from GaAs microstructures on Si](#)

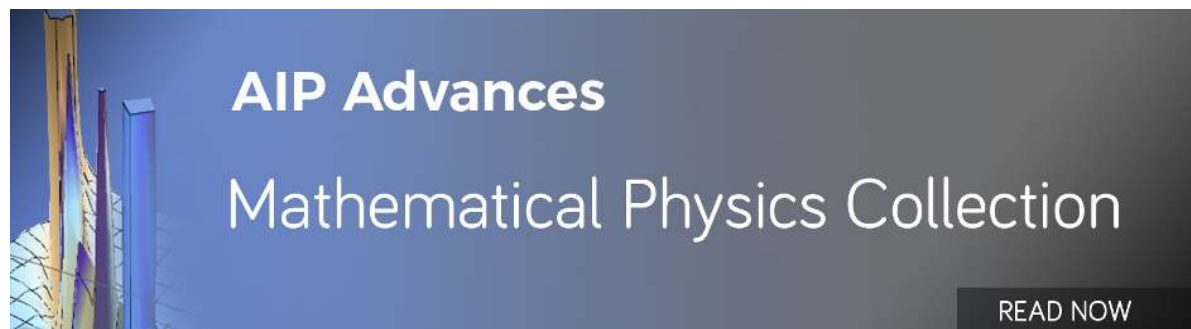
AIP Advances **8**, 125027 (2018); <https://doi.org/10.1063/1.5079668>

[High-efficiency optical terahertz modulation of aligned Ag nanowires on a Si substrate](#)

Applied Physics Letters **112**, 111101 (2018); <https://doi.org/10.1063/1.5008485>

[Failure of P-surfaced Shellular subjected to internal pressure](#)

AIP Advances **9**, 025010 (2019); <https://doi.org/10.1063/1.5066578>



Terahertz resonant transmission through metallic mesh truss structures

Cite as: AIP Advances 9, 125320 (2019); doi: 10.1063/1.5119385

Submitted: 10 July 2019 • Accepted: 7 December 2019 •

Published Online: 23 December 2019




View Online



Export Citation



CrossMark

Chul Kang,¹ Seong Han Kim,¹  Gyuseok Lee,¹ Inhee Maeng,¹ Seung Chul Han,² Kiju Kang,^{2,a)} and Chul-Sik Kee^{1,b)}

AFFILIATIONS

¹Integrated Optics Laboratory, Advanced Photonics Research Institute, Gwangju Institute Science and Technology, Gwangju 61105, South Korea

²School of Mechanical Engineering, Chonnam National University, Gwangju 61186, South Korea

^{a)}Electronic mail: kjkang@chonnam.ac.kr

^{b)}Electronic mail: cskee@gist.ac.kr

ABSTRACT

In mechanical engineering, truss structures have attracted much attention because of their mechanical strength and light weight. However, electromagnetic properties of truss structures have been rarely reported. We experimentally and numerically investigated a terahertz transmission through a truss structure composed of metallic meshes. In the experiments, a resonant transmission was observed through the metallic mesh truss structure. The frequencies and spatial distributions of the resonant modes were investigated in the numerical simulations. The frequencies of the resonant modes obtained from the numerical simulations agreed well with the observed frequencies. The field distributions of the resonant modes resemble those of the resonant modes of a Fabry–Perot resonator. Because truss structures are practically empty, they could be applied in realizing sensors to detect the chemical reactions of gases or molecular biomaterials in response to their changing refractive index.

© 2019 Author(s). All article content, except where otherwise noted, is licensed under a Creative Commons Attribution (CC BY) license (<http://creativecommons.org/licenses/by/4.0/>). <https://doi.org/10.1063/1.5119385>

Recently, in the field of mechanical engineering, much research has been conducted on light and elastic materials.^{1–8} Among them, truss structures are composed of a mesh having an extremely thin structure, and their size is easy to control; therefore, truss structures have been applied to large structures, such as legs in a nanosized structure. In addition, the thickness and weight of a material constituting a truss structure can be controlled to maintain the rigidity or increase the ductility intentionally. Another advantage of a truss structure is that it has a skeleton structure, and therefore, it is easy to access the cycle and height, and the structural characteristics can be predicted.

It has been reported that three-dimensional metallic wire structures can exhibit interesting electromagnetic (EM) properties such as a photonic band gap and extremely low-frequency plasmons.^{9,10} Metamaterials composed of metallic resonant structures exhibit numerous exciting EM properties and phenomena such as negative refractive index,¹¹ negative refraction,¹² magnetic response at a terahertz (THz) frequency,¹³ toroidal dipolar response,¹⁴ high

chirality,¹⁵ effective zero-refractive index,¹⁶ perfect absorption,¹⁷ and invisible cloaking.¹⁸ Thus, truss structures composed of metallic meshes can be expected to exhibit interesting EM properties. Moreover, owing to the mechanical flexible properties of the metallic mesh truss structures, it is possible to add new functional EM properties. However, the EM properties of the metallic mesh truss structures have been rarely studied.

Recently, manipulating THz radiation has attracted much attention because it can realize promising applications such as nondestructive evaluation, home security, biological and medical imaging, and THz communication. Modulation of the intensity or phase of a THz radiation can be realized using graphene,^{19–21} topological insulators,²² organic/inorganic hybrid materials,^{23,24} plasmonic structures,^{21,25,26} and metamaterials.^{21,27} A three-dimensional periodic structure composed of dielectric meshes has been proposed to manipulate THz radiation.^{28,29} Thus, the metallic mesh truss structures that respond to THz radiation could be useful in controlling it.

In this paper, THz transmission through a truss structure composed of nickel-tungsten alloy wires is studied via THz time-domain spectroscopy (THz-TDS). The metallic mesh truss structure exhibited a resonant transmission at certain frequencies. The numerical simulations revealed that the resonant modes resembled those of a Fabry–Perot resonator. A metallic mesh truss structure could be useful in implementing sensors for the detection of chemical reactions of gases, liquids, and biomedical materials occupying a structure. Furthermore, a metallic mesh truss structure with mechanical flexibility could act as a THz tunable filter and THz modulator.

A sample was fabricated based on a polymeric template with the out-of-plane truss elements formed by a mask-based lithography technique and the self-propagating photopolymer waveguide technique,¹ which was also used for Microlattice and Shellular.⁵ Following this, postprocesses (i.e., electroless plating of Ni–P, polishing, and etching) were sequentially performed to finally obtain the sample.

Figures 1(a) and 1(b) show the side and top views of the sample, respectively. The periodicity of the sample is about $1525\ \mu\text{m}$. The targeted thickness of the wire is $200\ \mu\text{m}$, but the sample has a thickness ranging from 200 to $260\ \mu\text{m}$, and the cross-angle between the wires viewed from the truncated side is about 45° . The measured height of the structure is about $3.5\ \text{mm}$ for the sample. The area of each entire sample is $8\ \text{mm} \times 10\ \text{mm}$.

A standard THz-TDS system was employed to measure the transmission THz pulses through the sample.³⁰ The schematic of the THz-TDS system is presented in Fig. 1(c). In the system, the pumping femtosecond-laser has a repetition rate of $82\ \text{MHz}$, central wavelength of $800\ \text{nm}$, and power of about $250\ \text{mW}$ after passing through a 3-mm pinhole and chopper. A p-type InAs wafer is used to generate a THz pulse, and a $5\text{-}\mu\text{m}$ dipole gap antenna on a low-temperature grown GaAs substrate is used to detect it. The truss structure is placed in the middle of the four parabolic mirrors on which the THz pulse is focused, and the full width half maximum of the focused THz pulse is about $2\ \text{mm}$. The sample is fixed to a 7-mm metal hole. The THz pulse is normally incident on the sample. To observe the resonance frequency of the sample accurately, a dry air-tight box is used during the measurements.

Figure 2(a) shows the measured data of the time-domain waveforms of the transmitted THz pulses through the sample and air. The time-domain data were measured in $150\ \text{ps}$ (inset), and the time step was $10\ \mu\text{m}/c$ ($\sim 0.033\ \text{ps}$), where c is the speed of light in air. The peak-to-peak value of the transmitted THz pulse through the sample is much smaller than that of the transmitted THz pulse through air because the sample composed of metal wires strongly reflects the THz pulse. Figure 2(b) shows the spectral amplitudes of the THz pulses transmitted through the sample and air. They are obtained from the time-domain waveforms via fast Fourier transformation. The amplitudes of the THz pulses were normalized to the maximum

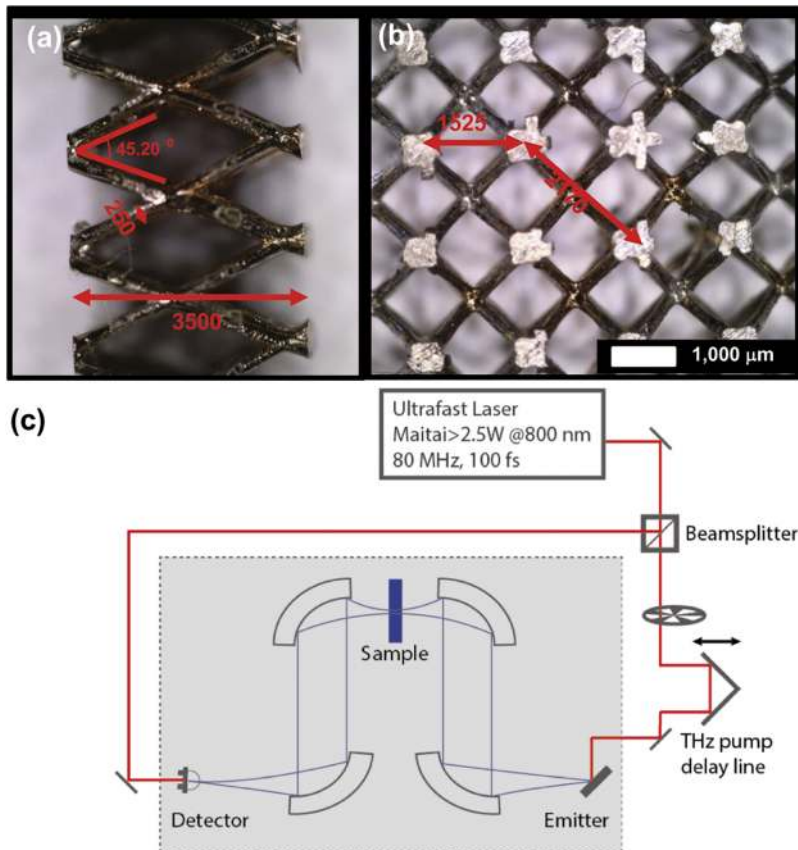


FIG. 1. Side (a) and top (b) views of the sample. Schematic view of the THz time-domain spectroscopy system employed in the experiments (c).

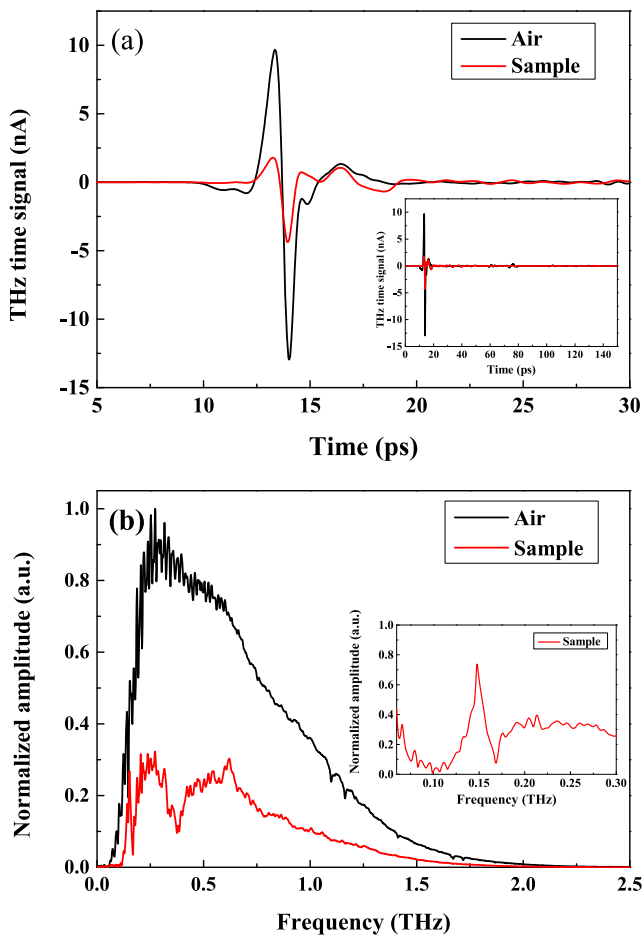


FIG. 2. Measured time-domain waveforms of the transmitted THz pulses through the sample (red) and air (black) (a) and their spectral amplitudes in the frequency domain (b). The insets in (a) and (b) represent the time-domain data measured for 150 ps and normalized spectral amplitude in the range from 0.05 to 0.30 THz, respectively. A resonant transmission through the sample is clearly observed around 0.15 THz.

amplitude of the THz pulse transmitted through air. The inset shows the transmitted amplitude of the THz pulse through the sample in the range from 0.05 to 0.30 THz. A resonant transmission is clearly observed around 0.15 THz.

Numerical calculations were performed to investigate the resonant transmittance. COMSOL Multiphysics was employed for the numerical calculations. Figure 3 shows the measured (black) and calculated (red) transmittance through the sample in a range of frequency from 0.11 to 0.18 THz. The calculated resonant transmittance around 0.15 THz is in good agreement with the measured resonant one. The resonant modes were investigated by numerical calculations. In fact, since the measured data are very noisy below 0.1 THz in our measurements, it is not possible to observe the resonant transmittance below 0.1 THz. However, the resonant modes below 0.1 THz can be observed in the calculated transmittance.

Figure 4(a) shows the calculated transmittance of a THz pulse through the sample. The calculated transmittance shows resonant

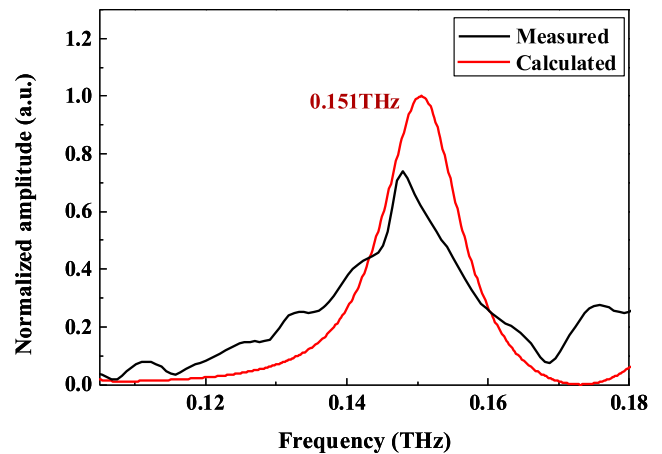


FIG. 3. Measured (black) and calculated (red) transmittance through the sample.

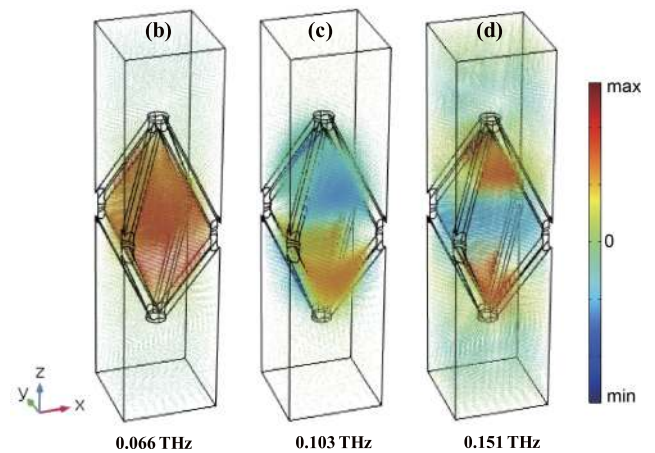
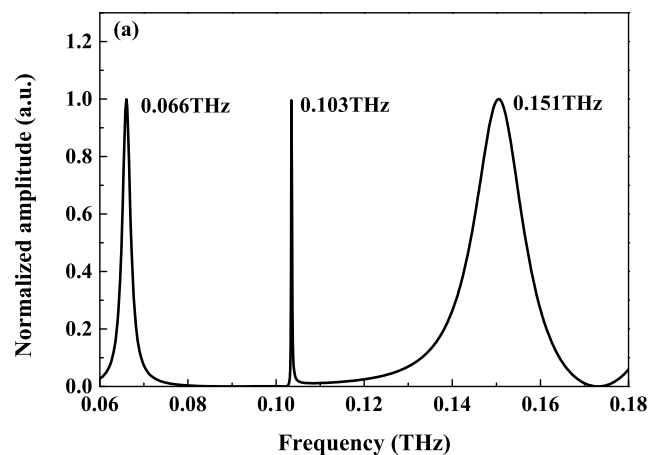


FIG. 4. Calculated transmittance through the sample (a) and spatial distributions of the resonant modes at 0.066 (b), 0.103 (c), and 0.151 THz (d) in a unit cell.

peaks at 0.066, 0.103, and 0.151 THz. Figures 4(b)–4(d) show the three-dimensional spatial distributions of the electric fields of the lowest third resonant modes of the sample at 0.066, 0.103, and 0.151 THz, respectively. The field distributions of the resonant modes resemble those of the resonant modes of a Fabry–Perot resonator, satisfying the relation between the length of the resonator, L , and resonant wavelength, λ_{re} , where $L = n\lambda_{re}/2$ and n is a positive integer.

Truss structures composed of metallic mesh wires can be easily compressed or stretched by an external force. So, the resonant transmittance frequencies of a sample are expected to increase under compression along the vertical direction of the sample because its height is reduced along the vertical direction. Furthermore, because truss structures are practically empty, they can be applied in realizing sensors to detect the chemical reactions of gases or molecular biomaterials in response to their changing refractive index.

In conclusion, the THz transmittance through a truss structure composed of metal wires is investigated experimentally and numerically. The truss structures can exhibit resonant transmittance. The calculated spatial distributions of the electric fields of the resonant modes and resonant frequencies show that their features resemble those of a Fabry–Perot resonator. Therefore, the truss structures may be applied in implementing filters and sensors owing to their structural properties.

This work was supported by the Gwangju Institute of Science and Technology (GIST) Research Institute (GRI) grant funded by the GIST in 2019 and Basic Science Research Program through the National Research Foundation of Korea (NRF) funded by the Ministry of Education (Grant Nos. NRF2018R1D1A1B07047762 and 2019R1F1A1063156) and the Ministry of Science and Information Communication Technology (Grant No. 2018R1A2A1A05023138).

REFERENCES

- ¹T. A. Schaedler, A. J. Jacobsen, A. Torrents, A. E. Sorensen, J. Lian, J. R. Greer, L. Valdevit, and W. B. Carter, *Science* **334**, 962 (2011).
- ²D. C. Jang, L. R. Meza, F. Greer, and J. R. Greer, *Nat. Mater.* **12**, 893 (2013).
- ³L. R. Meza, S. Das, and J. R. Greer, *Science* **345**, 1322 (2014).
- ⁴X. Zheng *et al.*, *Science* **344**, 1373 (2014).
- ⁵S. C. Han, J. W. Lee, and K. Kang, *Adv. Mater.* **27**, 5506 (2015).
- ⁶D. H. Choi, M. G. Lee, S. C. Han, Y. C. Jeong, J. S. Cho, and K. Kang, *Int. J. Mech. Sci.* **149**, 311 (2018).
- ⁷S. C. Han, J. M. Choi, G. Liu, and K. Kang, *Sci. Rep.* **7**, 13405 (2017).
- ⁸X. Yu, J. Zhou, H. Liang, Z. Jiang, and L. Wu, *Prog. Mater. Sci.* **94**, 114 (2017).
- ⁹D. F. Sievenpiper, M. E. Sickmille, and E. Yablonovitch, *Phys. Rev. Lett.* **76**, 2480 (1996).
- ¹⁰J. B. Pendry, A. J. Holden, W. J. Stewart, and I. Youngs, *Phys. Rev. Lett.* **76**, 4773 (1996).
- ¹¹V. Veselago, *Sov. Phys.-Usp.* **10**, 509 (1968).
- ¹²R. A. Shelby, D. R. Smith, and S. Schultz, *Science* **292**, 77 (2001).
- ¹³T. J. Ye, W. J. Padilla, N. Fang, D. C. Vier, D. R. Smith, J. B. Pendry, D. N. Basov, and X. Zhang, *Science* **303**, 1494 (2004).
- ¹⁴T. Kaelberer, V. Fedotov, N. Papisimakis, D. Tsai, and N. Zheludev, *Science* **330**, 1510 (2010).
- ¹⁵J. K. Gansel, M. Thiel, M. S. Rill, M. Decker, K. Bade, V. Saile, G. Freymann, S. von Linden, and M. Wegener, *Science* **325**, 1513 (2009).
- ¹⁶P. Moitra, P. Yang, Z. Anderson, I. I. Kravchenko, D. P. Briggs, and J. Valentin, *Nat. Photonics* **7**, 791 (2013).
- ¹⁷N. I. Landy, S. Sajuyigbe, J. J. Mock, D. R. Smith, and W. J. Padilla, *Phys. Rev. Lett.* **100**, 207402 (2008).
- ¹⁸D. Schurig, J. J. Mock, B. J. Justice, S. A. Cummer, J. B. Pendry, A. F. Starr, and D. R. Smith, *Science* **314**, 977 (2006).
- ¹⁹Z. Miao, Q. Wu, X. Li, Q. He, K. Ding, Z. An, Z. Zhang, and L. Zhou, *Phys. Rev. X* **5**, 041027 (2015).
- ²⁰S. H. Lee, M. Choi, T. T. Kim, S. Lee, M. Liu, X. Yin, H. K. Choi, S. S. Lee, C.-G. Choi, X. Zhang X, and B. Min, *Nat. Mater.* **11**, 936 (2012).
- ²¹M. Rahm, J.-S. Li, and W. J. Padilla, *J. Infrared, Millimeter, Terahertz Waves* **34**, 1 (2013).
- ²²C. In, S. Sim, B. Kim, H. Bae, H. Jung, W. Jang, M. Son, J. Moon, M. Salehi, S. Y. Seo, A. Soon, M.-H. Ham, H. Lee, S. Oh, D. Kim, M.-H. Jo, and M.-H. Choi, *Nano Lett.* **18**, 734 (2018).
- ²³H. K. Yoo, Y. Yoon, K. Lee, C. Kang, C.-S. Kee, I.-W. Hwang, and J. W. Lee, *Appl. Phys. Lett.* **105**, 011115 (2014).
- ²⁴H. K. Yoo, S.-G. Lee, C. Kang, C.-S. Kee, and J. W. Lee, *Appl. Phys. Lett.* **103**, 151116 (2013).
- ²⁵J. W. Lee, J.-K. Yang, I.-B. Sohn, H. K. Yoo, C. Kang, and C.-S. Kee, *Opt. Express* **22**, 18433 (2014).
- ²⁶M. Seo, J. Kyoung, H. Park, S. Koo, H.-S. Kim, H. Bernien, B. J. Kim, J. H. Choe, Y. H. Ahn, H.-T. Kim, N. Park, Q.-H. Park, K. Ahn, and D.-S. Kim, *Nano Lett.* **10**, 2064 (2010).
- ²⁷H.-T. Chen, W. J. Padilla, J. M. O. Zide, A. C. Gossard, A. J. Taylor, and R. D. Averitt, *Nature* **444**, 597 (2006).
- ²⁸M. C. Wanke, O. Lehmann, K. Müller, Q. Wen, and M. Stuke, *Science* **275**, 1284 (1997).
- ²⁹C. R. Tubío, J. A. Nóvoa, J. Martin, F. Guitian, J. R. Salgueiro, and A. Gil, *RSC Adv.* **6**, 2450 (2016).
- ³⁰J.-K. Yang, C. Kang, I. Sohn, and C.-S. Kee, *Opt. Express* **18**, 25371 (2010).